INVESTIGATION INTO THE KINETICS OF AEROSOL FORMATION AT PHOTOLYSIS OF THE TUNGSTEN CARBONYL $W(CO)_6$

S.N. Dubtsov, G.I. Skubnevskaya, A.I. Levykin, and K.K. Sabel'feld

Institute of Chemical Kinetics and Combustion,
Siberian Branch of the Russian Academy of Sciences, Novosibirsk
Computer Center,
Siberian Branch of the Russian Academy of Sciences, Novosibirsk
Received February 4, 1998

Kinetics of formation and growth of finely disperse aerosol at tungsten carbonyl photolysis in air is studied experimentally. The emphasis is on the effect of coagulation and the interval between termination of the generation and the time of particle detection (t_1) on the measured concentration and the particle size distribution. Kinetics of aerosol formation is numerically simulated within the framework of the Smolukhovskii coagulation model. The rate of generation of condensing products, "monomers" $F(t)$, was derived from comparison between the experimental and calculated data. The derived value proves to agree well with the independently measured rate of $W(CO)_6$ photolysis.

1. INTRODUCTION

Investigation into the processes of disintegration of carbonyls of transient metals remains urgent for the last decades. This is caused by the use of materials based on them in catalysis,[1] radio electronics,[2] etc. Much attention is paid to the study of UV and IR photolysis of carbonyls.[3–5] Products of carbonyl photolysis – atoms or metal oxides (in the presence of oxygen) – can transit into the aerosol state. In this paper, kinetics of photochemical formation of $W(CO)_6$ aerosol is studied in detail, and dynamics of this process is simulated numerically within the framework of the Smolukhovskii coagulation model. Our main concern was with an increase in reliability and accuracy of the algorithm for calculation of the rate of generation of the condensing molecules ("monomers").

2. EXPERIMENT

Kinetics of aerosol formation at $W(CO)_6$ photolysis was experimentally studied in a through-type system similar to that described earlier in Ref. 6. The air flow, purified with an aerosol filter and a column with a molecular sieve 4A, passed through the thermostatic U-shaped tube at 25°C. The tube contained crystal $W(CO)_6$ and the air flow became saturated with the carbonyl vapor. The resulting vapor-air mixture came to the Quartz through-type reactor of the laminar type. Vapor of reagents were irradiated with full light of a mercury lamp DRSh–500. Radiation intensity varied by changing the distance from the lamp to the reactor. The irradiation time, t_0, varied within the interval 0.03–15 s with the use of a slit diaphragm set in front of the reactor. The interval between termination of the photolysis and the time of particle detection (the delay time), t_1, changed from 3.5 to 386 s by setting additional through-type flasks.

The particle number density and size distribution were measured by an automated aerosol spectrometer within the ranges form 10^2 to 10^7 particle/cm^3 and from 2 to 200 nm size, respectively.

3. EXPERIMENTAL RESULTS

3.1. Kinetics of the photochemical aerosol formation

The simplified mechanism of the tungsten carbonyl photolysis in the presence of oxygen can be presented as the following chain of reactions[8]:

$$W(CO)_6 \xrightarrow{h\nu} W(CO)_5 +$$

$$+ CO \xrightarrow{O_2} W(CO)_4 \xrightarrow{O_2} \ldots \rightarrow WO_x,$$

where $x = 2, 3$. The resulting product is the mixture of WO_2 and WO_3, just that which forms aerosol particles. Figure 1 presents the aerosol particle number density as a function of the irradiation time.

It should be noted that new monomer molecules are not generated in the interval t_1. In this time, condensation and coagulation of already formed monomers and clusters take place. As a result, aerosol

0235-6880/98/10 969-04 $02.00

particle number density and size distribution are different in the reactor and at the measurement point. Figure 2 presents the experimental dependence of N_a on t_0 for different values of t_1.

As seen from the figure, at short t_0 (and small N_a) the particle number density increases with increasing t_1. Conversely, at $t_0 > 4$ s it decreases with increasing t_1. That is why the value of t_1 should be taken into account when analyzing the nucleation kinetics for calculation of the rate of monomer generation.

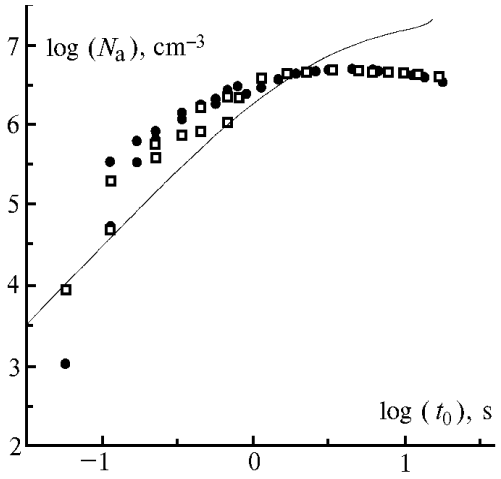

FIG. 1. Particle number density vsx the irradiation time for t_1=3.5 s. [W(CO)$_6$]=1.13·10^{13} cm^{-3}. Experimentally measured W_{phot} = 1.69·10^9 cm^{-3}·s^{-1}, calculated $F(t)$ = 1.16·10^9 cm^{-3}·s^{-1}. Dots are for experimental data, the curve is for the calculated results.

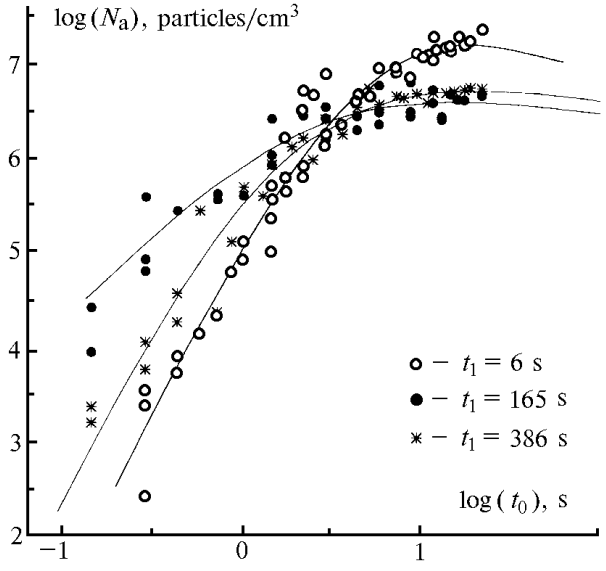

FIG. 2. Particle number density vsx the irradiation time for different values of t_1 and W_{rel} = 4·10^{-4}. Dots are for experimental data, curves are for results of numerical simulation.

3.2. Numerical model

In order to find the rate of monomer generation $F(t)$, we have calculated numerically the kinetics of aerosol formation within the framework of the Smolukhovskii coagulation model in the mode of free molecular collision of clusters, similar to that described in Ref. 8. Earlier the authors have developed an efficient algorithm for solution of the coagulation equation.[6,9] In this work, the model is modified so that it takes into account the influence of t_1 and aerosol sedimentation on the reactor surface. Similarly to Ref. 8, the main assumptions in this model are as follows:

1) the rate of monomer generation $F(t)$ is constant;

2) all collisions of monomers and clusters result in the formation of new clusters;

3) there is no evaporation of monomers from the surface of aerosol particles.

In this case, concentration of monomers and clusters varies in time in accordance with the following equations:

$$\frac{dN_1}{dt} = -N_1 \sum_{i=1}^{\infty} \beta_{1i} N_1 + F(t) - \gamma_1 N_1, \quad (1)$$

$$\frac{dN_k}{dt} = \frac{1}{2} \sum_{i+j=k}^{\infty} \beta_{ij} N_i N_j - N_k \sum_{i=1}^{\infty} \beta_{ki} N_i - \gamma_k N_k; \quad (2)$$

$F(t) = F$ = const at $t \ge \tau_0$, $F(t) = 0$ at $\tau_0 \le t \le \tau_0 + \tau_1$, where N_1 and N_k are the concentrations of monomers and clusters consisting of k monomers; β_{ij} is the gas-kinetic constant of collision of clusters consisting of i and j monomers; γ_i is the constant of sedimentation of ith cluster upon the reactor surface. Following Ref. 8, let us consider the substitution of variables:

$$N_i = k_n n_i \; t = k_\tau \tau, \quad (3)$$

where $k_n = (F/\beta_{11})^{1/2}$, $k_\tau = (1/F\beta_{11})^{1/2}$.

Then, the set of eCuations (1)–(2) takes the following form:

$$dn_1/d\tau = \tilde{F} - n_1 \sum_{i=1}^{\infty} K_{1i} n_i - \tilde{\gamma}_1 n_1, \quad (4)$$

$$dn_k/d\tau = 1/2 \sum_{i+j=k} K_{ij} n_i n_j - n_k \sum_{i=1}^{\infty} K_{ki} n_k - \tilde{\gamma}_k n_k; \quad (5)$$

$$\tilde{F}(\tau) = 1 \text{ at } \tau \le \tilde{\tau} \le \tilde{\tau} + \tau_1,$$

$$\tilde{F}(\tau) = 0 \text{ at } \tilde{\tau}_0 \le \tilde{\tau} \le \tilde{\tau}_0 + \tilde{\tau}_1,$$

where $\tilde{\tau}_0 = \tau_0/k_\tau$, $\tilde{\tau}_1 = \tau_1/k_\tau$, $\tilde{\gamma}_1 = \gamma_k/k_\tau$, $K_{ij} = \beta_{ij}/\beta_{11}$. In the case of free molecular collisions,

$$K_{ij} = 1/4\sqrt{2}\,(i^{1/3} + j^{1/3})^2\,(1/i + 1/j)^{1/2}. \quad (6)$$

To solve the Cauchy problem presented by Eqs. (4)–(5), the section finite-element algorithm proposed by the authors was applied. This algorithm uses 50 point and 80 cubic finite elements for approximation of the aerosol particle number density spectrum. Experimental data and the calculated curves were compared similarly to the method given in Ref. 6.

Since Eqs. (4)–(5) contain the unknown value k_τ, the theoretical kinetic curves were calculated by iterations, but with refinement of the k_τ value at each iteration. For given k_τ, the values of $\tilde{\tau}_1$ and $\tilde{\gamma}_1$ were calculated, and the solution of Eqs. (4)–(5) were found for $10^{-2} \le \tau_0 \le 30$ and calculated $\tilde{\tau}_1$ and $\tilde{\gamma}_1$. Then the temporal dependence $\tilde{N}_J(\tau_0) = \sum_{l=J}^{\infty} n_l(\tau_0)$ of the total number density of clusters of the size $l \ge J$ on τ_0 was found for a given J. Selecting the same scales on logarithmic scale along the vertical and horizontal axes, we used the parallel transfer of the experimental points (δ_y along the y-axis and δ_x along the x-axis) for those to be maximally close to the calculated curve. The parameters δ_y and δ_x were found by minimizing the functional:

$$\Phi_J(\delta_y, \delta_x) = \sum_{i=1}^{20} (y_i + \delta_i - \phi(x_i + \delta_x))^2,$$

where y_i and x_i are the logarithms of the parameters $N_J(t)$ and $t(t)$; $N_J(t) = \sum_{l=J}^{\infty} n_l(t)$ is the experimentally measured total number density of clusters of the size $l \ge J$; $\varphi(x)$ is the value at the point x of the spline reconstructed from the calculated data $\tilde{N}_J(\tau_0)$. Then a new value of $k_\tau = 10^{\delta_x}$ is calculated.

This procedure started with the initial value $k_\tau = 1$. It repeated until k_τ coincides with the preceding value accurate to two significant digits. Usually 3–4 iterations were enough; further k_τ stopped to refine. The monomer generation rate $F(t)$ can be estimated as $F(t) = k_n / k_\tau \approx 10^{\delta_y - \delta_x}$.

4. DISCUSSION

One of the main problems of numerical modeling of the nucleation kinetics is the calculation of the value of $F(t)$. In this paper, the additional parameter t_1 is taken into account in the model.

As noted above, to calculate $F(t)$, it is necessary, first, to estimate the minimal detectable value J from the minimum of the functional Φ_J. The Table I gives a number of Φ_J values calculated for different t_1 and J using the experimental data from Fig. 2.

As seen from the Table, Φ_J is minimal at $J = 5$. This means that detectable are particles consisting of 5 and more monomers. The numerical modeling shows that, if the accuracy of J determination is ± 1, then this results in a ± 30% uncertainty in $F(t)$ calculation. Besides, the greater t_1 and spread in experimental data, the weaker J dependence of Φ_J and the greater error in the $F(t)$ determination.

TABLE I. The values of the functional $\Phi_J \times 0.1$ *for different* t_1 *and* J.

t_1	6	40	165	386
J	Φ_J	Φ_J	Φ_J	Φ_J
2	0.600	0.381	0.249	0.217
4	0.223	0.130	0.159	0.342
6	0.288	0.194	0.150	0.406
10	0.602	0.386	0.159	0.472

The constant of $W(CO)_6$ photolysis was measured independently, the rate of photolysis W_{phot} was determined for the conditions of the experiment (see Fig. 1). We have found $W_{phot} = 1.69 \cdot 10^9$ cm^{-3}·s^{-1}. The value calculated from the model is $F(t) = 1.16 \cdot 10^9$ cm^{-3}·s^{-1}. Thus, the experimentally measured rate of $W(CO)_6$ photolysis coincides with the rate of monomer generation calculated from the model. If $F(t)$ is calculated neglecting t_1, then the resulting value is $5.41 \cdot 10^8$ cm^{-3}·s^{-1}. So, the neglect of t_1 in $F(t)$ calculation results in large errors.

CONCLUSIONS

Influence of coagulation and the delay time t_1 on the formation kinetics of aerosol particles of the nanometer size range at tungsten carbonyl photolysis has been studied.

The kinetics of $W(CO)_6$ aerosol formation has been modeled numerically within the framework of the modified Smolukhovskii coagulation model accounting for the value of t_1.

The rate $F(t)$ of generation of the condensing products closely coincides with the independently measured rate of $W(CO)_6$ photolysis. Thus, it is shown that the account for t_1 increases the reliability of $F(t)$ reconstruction.

ACKNOWLEDGMENTS

This work was supported in part by the Russian Foundation for Basic Researches, Grant No. 96–03–33304a.

REFERENCES

1. F.A. Cotton and G. Wilkinson, in: *Advanced Inorganic Chemistry*, 5th ed. (Wiley, New York, 1988), pp. 1224–1282.

2. J. Haigh, K. Blake, and G. Burkhardt, J. Crystal Growth. **155**, 266–271 (1995).

3. Z. Karny, R. Naman, and R.N. Zare, Chem. Phys. Lett. **59**, 33–37 (1978).
4. D.P. Gerrity, L.J. Rolhberg, V. Vaida, Chem. Phys. Lett. **74**, No. 1, 1–5 (1980).
5. S. Trushin, K. Sugawara, and H. Takeo, Chem. Phys. **203**, 267–278 (1996).
6. S.N. Dubtsov, K.P. Koutzenogii, A.I. Levykin, and G.I. Skubnevskaya, J. Aerosol Sci. **26**, 705–717 (1995).
7. V.N. Fomin, Zh. Obshch. Khimii **65**, No. 7, 1092–1095 (1995).
8. N.P. Rao and P.H. McMurry, Aerosol Sci. Technol. **11**, 120–132 (1992).
9. Dubtsov, K.P. Koutzenogii, A.I. Levykin, K.K. Sabel'feld, and G.I. Skubnevskaya, Dokl. Akad. Nauk RAN **330**, 327–331 (1993).